Heliyon 10 (2024) e31424

Contents lists available at ScienceDirect

Heliyon

journal homepage: www.cell.com/heliyon

Research article

Harnessing bio-based chelating agents for sustainable synthesis of AgNPs: Evaluating their inherent attributes and antimicrobial potency in conjunction with honey

Muneeb Irshad [a,**], Anum Mukhtar [a,1], Asif Nadeem Tabish [b], Muhammad Bilal Hanif [c,1,*], Mahshab Sheraz [k], Viktoriia Berezenko [c,j], Muhammad Zubair Khan [d], Farwa Batool [a], Muhammad Imran [e], Muhammad Rafique [f], Jacek Gurgul [g], Thamraa Alshahrani [h], Michał Mosiałek [g], Juran Kim [k,l,***], Richard T. Baker [i], Martin Motola [c,****]

[a] *Department of Physics, University of Engineering and Technology, Lahore, 54890, Pakistan*
[b] *Department of Chemical Engineering, University of Engineering and Technology, New Campus, Lahore, 39021, Pakistan*
[c] *Department of Inorganic Chemistry, Faculty of Natural Sciences, Comenius University Bratislava, Ilkovicova 6, Mlynska Dolina, 842 15, Bratislava, Slovakia*
[d] *Pak-Austria Fachhochschule: Institute of Applied Sciences and Technology Mang, Haripur, 22621, KPK, Pakistan*
[e] *Department of Parasitology, University of Veterinary and Animal Sciences, Lahore, Pakistan*
[f] *Department of Physics, University of Sahiwal, 57000, Sahiwal, Pakistan*
[g] *Jerzy Haber Institute of Catalysis and Surface Chemistry, Polish Academy of Sciences, Niezapominajek 8, PL–30239 Krakow, Poland*
[h] *Department of Physics, College of Sciences, Princess Nourah Bint Abdulrahman University (PNU), P.O. Box 84428, Riyadh, 11671, Saudi Arabia*
[i] *School of Chemistry, University of St. Andrews, St. Andrews, Fife, KY16 9AJ, United Kingdom*
[j] *Department of Environmental Ecology and Landscape Management, Faculty of Natural 11 Sciences, Comenius University Bratislava, Ilkovicova 6, 842 15, Bratislava, Slovakia*
[k] *Advanced Textile R&D Department, Korea Institute of Industrial Technology (KITECH), Ansan-si, 15588, Republic of Korea*
[l] *HYU-KITECH Joint Department, Hanyang University, 222, Wangsimni-ro, Seongdong-gu, Seoul, 04763, Republic of Korea*

ARTICLE INFO

Keywords:
AgNP
Chelating agent
Honey
Escherichia coli
Anti-bacterial applications

ABSTRACT

Greenly synthesized nanoparticles have garnered attention due to their low environmental footprint, but impurities limit their applications. A novel semi-organic method for synthesizing silver nanoparticles (AgNPs) using bio-based chelating fuels (*Beta vulgaris* subsp., *Spinacia oleracea, and Ipomoea batatas*) reduces the undesirable impurities. The study also showcases the impact of bio-based chelating fuel on various characteristics of AgNPs in comparison to synthetic chelating fuel. The antimicrobial efficacy of the synthesized AgNPs in conjunction with honey was also assessed against *E. coli.* The XRD analysis showed cubic structure of AgNPs. The FESEM and

* Corresponding author. Department of Inorganic Chemistry, Faculty of Natural Sciences, Comenius University Bratislava, Ilkovicova 6, Mlynska Dolina, 842 15, Bratislava, Slovakia.
** Corresponding author.
*** Corresponding author. Advanced Textile R&D Department, Korea Institute of Industrial Technology (KITECH), Ansan-si, 15588, Republic of Korea.
**** Corresponding author.
E-mail addresses: muneebirshad@gmail.com (M. Irshad), hanif1@uniba.sk, bilalhanif46@gmail.com (M. Bilal Hanif), jkim0106@kitech.re.kr (J. Kim), martin.motola@uniba.sk (M. Motola).
[1] Equal contribution.

https://doi.org/10.1016/j.heliyon.2024.e31424
Received 16 January 2024; Received in revised form 15 May 2024; Accepted 15 May 2024
Available online 16 May 2024

TEM analysis showed that the well-connected spherical-shaped AgNPs (~3–120 nm diameter) while EDS confirmed the presence of Ag in all samples. The TEM analysis also revealed layers of carbonates in AgNPs synthesized using bio-based chelating fuels. XPS investigation confirmed the absence of any prominent impurities in prepared samples and AgNPs have not experienced oxidation on their surface. However, notable surface charging effects due to the uneven conductivity of the particles were observed. The broth dilution method showed that all mixtures containing AgNPs in combination with honey exhibited a significant bacterial growth reduction over a period of 120 h. The highest growth reduction of ~75 % is obtained for the mixture having AgNPs (*Ipomoea batatas*) while the least growth reduction of ~51 % is obtained for the mixture having AgNPs (Beta vulgaris subsp.). The findings affirm that AgNPs can be successfully synthesized using bio-based chelating fuels with negligible ecological consequences and devoid of contaminants. Moreover, the synthesized AgNPs can be employed in conjunction with honey for antibacterial purposes.

1. Introduction

Nanotechnology a diverse interdisciplinary research field, provides innovative solutions to various aspects of human life [1,2]. Nanomaterials exhibit promising biological, mechanical, and thermal properties in contrast to their basic form owing to their large surface area to size ratio and quantum effect [3,4]. Researchers have developed a wide range of deliberate manufacturing techniques to enhance the overall properties of nanomaterials. Nowadays, nanoparticles are employed in various aspects of the biomedical field, such as medicine, biosensing, drug delivery, and nanodevices [5,6].

Silver nanoparticles (AgNPs) have been of great interest to researchers because of their anti-bacterial, anti-viral, and anti-fungal properties. AgNPs can penetrate the cell walls and modify the cell membrane structure of bacteria, leading to their death [7,8]. The penetration ability of AgNPs depends on the shape, size, crystal structure, concentration, and surface zeta potential of the AgNPs. These properties allow AgNPs to have anti-bacterial properties without generating bacterial resistance compared to conventional antibiotics [9,10].

Besides AgNPs, honey a naturally occurring product also carries a wide array of antimicrobial properties. Honey is used against microbiological diseases since ancient times and shows strong anti-bacterial activity against various human diseases, such as *Escherichia coli, Salmonella typhimurium, Enterobacter aerogenes, Staphylococcus aureus* etc. [11–13]. Honey's high osmolarity, acidity, and synthesis of H_2O_2 (peroxide) make it better for antibacterial and antioxidant applications [14,15]. One essential component of honey that exerts antibacterial activity against clinically significant pathogenic microorganisms is osmosis as honey is primarily comprised of fructose and glucose due to which honey dehydrates the bacteria upon contact and inhibits its growth [16]. The low content of water (less than 20 %) in honey does not allow bacteria to thrive as bacteria rely on water for metabolic processes. In addition, honey has flavonoids, phenolic acids, and enzymes that possess phytochemical and antioxidant qualities which enhance the anti-bacterial activity by neutralizing free radicals and disrupting the activities of bacterial cells [14,16]. The current project aims to utilize the synergetic role of both honey and AgNPs against *E. coli.* bacteria.

Unlike honey which occurs naturally, AgNPs must be synthesized either through a chemical approach or a green approach. In the chemical approach, AgNPs can be synthesized by a plethora of techniques such as sol gel, combustion, co-precipitation, solid state reactions, and hydrothermal routes using metallic precursors, chemical reducing agents, and stabilizing agents. However, chemical synthesis is not eco-friendly due to the presence of hazardous by-products [17,18]. During the last decade, eco-friendly green synthesis routes have been extensively employed to synthesize AgNPs. The biomolecules in organic extracts interact with the metal ions in a solution and reduce metal ions to their corresponding metal nanoparticles by donating electron. Furthermore, biomolecules can also stabilize the nanoparticles by binding to their surfaces through electrostatic or covalent interactions, preventing them from aggregating and stabilizing their size and shape [19,20]. Biomolecules also play a significant role in antimicrobial activity by employing their antibacterial, antifungal, and antiviral properties through several mechanisms, including disruption of cell membrane integrity, inhibition of essential metabolic pathways, and modulation of the immune response resulting in the growth reduction of bacteria [21]. Nevertheless, major drawbacks of green synthesis include its time-consuming nature, lack of reproducibility, and the existence of a high number of contaminants that might affect the fundamental features of the AgNPs [22–24]. In this study, a novel semi-organic combustion method was developed to synthesize AgNPs with low hazardous impact and impurities. The method uses organic fuel and biomolecules as reducing and capping agents in a solution containing metal precursors.

Beta vulgaris subsp.*, Spinacia oleracea* and *Ipomoea batatas* used in the current project not only possess biomolecules but also high concentrations of natural oxalic acid. Synthetic oxalic acid is widely used as a chelating and capping agent for the chemical synthesis of nanoparticles, however, there is increasing interest in developing bio-based alternatives due to their potential sustainability benefits. The semi-organic synthesis process using *Beta vulgaris* subsp.*, Spinacia oleracea* and *Ipomoea batatas* exploit the synergetic role of biomolecules and organic oxalic acid as reducing and capping agents therefor providing better control over the synthesis of nanoparticles. However, to remove the organic compounds, high calcination, and sintering temperatures are required [25,26].

This current study aims to synthesize AgNPs by utilizing the synergy of both biomolecules and bio-based chelating agents therefore resulting in lower ecological impact in contrast to chemical synthesis and lower impurities in the final product compared to green synthesis. In addition, the AgNPs synthesized with a semi-organic approach and in combination with honey will be used as an antibacterial agent against *E. coli.*

2. Experimentation

2.1. Materials

Silver nitrate (Merck, 99 %) was used as a precursor material. Synthetic oxalic acid was used as a chelating agent for the preparation of AgNPs by the chemical auto-combustion approach and *Beta vulgaris* subsp. *(Beetroot)*, *Spinacia oleracea (Spinach)* and *Ipomoea batatas (Sweet potato)* were used as bio-chelating agents for the semi-organic synthesis route.

The *Beta vulgaris* subsp, *Spinacia oleracea,* and *Ipomoea batatas* were acquired from nearby market and thoroughly rinsed multiple times with distilled water to eliminate any dust or particles adhering to their surfaces. The vegetables were then peeled with a peeler and cut into small pieces using a kitchen knife. The pieces were then again washed with distilled water multiple times and dried under natural sunlight for 48 h. Subsequently, a mortar and pestle was used to ground them into powder.

Honey was extracted from a fresh hive while freshly grown pure cultures of *Escherichia coli* were developed by the Department of Microbiology and the Department of Parasitology at the University of Veterinary and Animal Sciences (UVAS). All glassware was properly rinsed with distilled water and dried in the oven before use.

2.2. Synthesis of AgNPs

To synthesize AgNPs through a semi-organic route, silver nitrate (50 g) was added to distilled water (150 ml) and stirred for 20 min at 70 °C until a transparent solution was obtained. Then the prepared powder (20 g each) of *Beta vulgaris* subsp.*(Beetroot)*, *Spinacia oleracea (Spinach)* and *Ipomoea batatas (Sweet potato)* were added as a bio-chelating agent, and the solution was stirred further at 110 °C until a gel was formed. The gel was then subjected to further heating, in a furnace at 150 °C igniting auto-combustion and resulting in the formation of AgNPs. The obtained powder was calcined in an oven and the calcined powder was then grinded with a mortar pestle (Fig. 1(e)).

In the chemical approach, synthetic oxalic acid was used as a chelating agent. The above procedure was followed and AgNPs were obtained in the same manner, however, the formation of gel in a semi-organic approach took place after a longer period (20–30 min) compared to the chemical approach. The AgNPs synthesized by both routes were then sintered at 750 °C for 2 h to obtain the crystalline phase.

In the final step, the AgNPs synthesized using both routes were mixed with honey in a ratio of 0.6:1 i.e. 6g of AgNPs were mixed in 10g of honey, respectively. Subsequently, a quantity of 2 g from mixtures (honey + AgNPs synthesized using each respective method), was subjected to antimicrobial activity testing.

2.3. Characterization

X-ray diffraction (XRD, Malvern B.V., Lelyweg 1, Netherlands) was used for the structural analysis of the AgNPs, while their microstructures were analyzed by FESEM (MIRA3 TESCAN). The elemental composition of AgNPs was determined by EDS. XPS studies

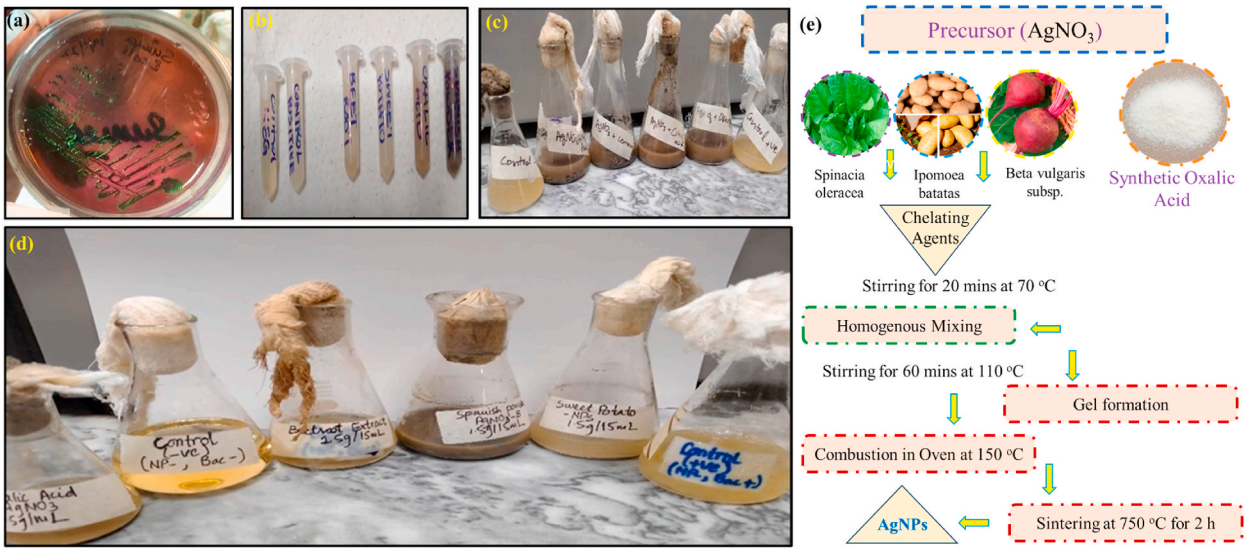

Fig. 1. Metallic sheen obtained after culturing *E. coli* on Eosin Methylene blue agar **(a)**. Color change of broth solution after addition of AgNPs (synthesized using *Beta vulgaris* subsp., *Spinacia oleracea, Ipomoea batatas*, and oxalic acid as chelating fuel) in combination with honey **(b–d)** along with the schematic for the synthesis route. (For interpretation of the references to colour in this figure legend, the reader is referred to the Web version of this article.)

were conducted in a multi-chamber ultra-high vacuum (UHV) system equipped with a SES R4000 (Gammadata Scienta) energy analyzer. All details about the UHV system, sample preparation, and XPS measurements can be found in reference [22]. TEM images were recorded using a Titan Themis 200 keV (FEI) transmission and scanning transmission electron microscope (S/TEM). For TEM analysis, the samples were suspended in acetone by ultrasonication and deposited onto holey carbon-coated Cu grids.

2.4. Antimicrobial activity test

Anti-bacterial activities of AgNPs (synthesized through each route) and honey were examined by a standard minimum inhibitory concentration (MIC) test using control-positive (with *E. coli*) and control-negative bacteria (without *E. coli*).

2.4.1. Broth dilution test

The broth dilution test is designed to determine the minimum inhibitory concentration (MIC) of the synthesized AgNPs in terms of their anti-bacterial attributes, which inhibit the growth of the tested bacteria. MIC values assesses the effectiveness of antimicrobial characteristics and therapeutic properties of the drug, and to evaluate the susceptibility of bacteria [25,26]. The antibacterial activity was tested by broth dilution method using Luria Bertani broth with 2 g of the antimicrobial agent (AgNPs in combination with honey). For broth dilution, bacteria were introduced into a liquid growth medium having antimicrobial agent. After incubation for a pre-determined time (20–24 h), growth is assessed, and the MIC value is recorded. The procedure was completed in five days (120 h) and involved only aerobic microorganisms.

2.4.2. Culturing and sub-culturing of Escherichia coli (E. coli.)

The culture plate containing *E. coli* was refreshed for active growth on the LB agar plate. The LB agar medium was prepared and autoclaved at 121 °C/15 psi, and afterward, LB agar plates were poured and solidified. Discrete *E. coli.* colonies were obtained by quadrat streaking and incubated at 37 °C for 24 h.

The presence of *E. coli.* culture was confirmed when it was cultured on Eosin Methylene blue Agar (EMB) and discrete colonies with a characteristic metallic sheen were obtained, as shown in Fig. 1(a–d) confirming the positive growth of *E. coli*. To observe the optical density of antibacterial activity (OD value), a LB solution was prepared and autoclaved. The 30 ml of LB solution was inoculated with "*E. coli*" bacteria (50 μl) and designated as control positive, while the control negative contained 30 ml of LB solution without any bacteria. To test the antibacterial activity of AgNPs, 10 ml of broth solution was taken in four flasks. In each flask, 2 g mixtures of AgNPs (synthetic oxalic acid) + honey, AgNPs (*Beta vulgaris* subsp.) + honey, AgNPs (*Ipomoea batatas*) + honey, and AgNPs (*Spinacia oleracea*) + honey were added, respectively. These flasks were incubated in the submerged shaker at 220 rpm/37 °C for proper aeration. An *E. coli* inoculum (50 μl) from a fresh overnight culture (primary culture) was added to each flask, which was then placed in a shaking incubator at 37 °C at 220 rpm for another 120 h. OD values were taken every 24 h using a spectrophotometer.

The percentage reduction growth was calculated from the control positive, control negative, and optical density (OD) values using equations (1) and (2), respectively.

$$\text{Relative growth } (\%) = \frac{OD - Control\ Negative}{Control\ Postive} \times 100 \tag{1}$$

$$\text{Reduction growth } (\%) = 100 - Relative\ growth\ (\%) \tag{2}$$

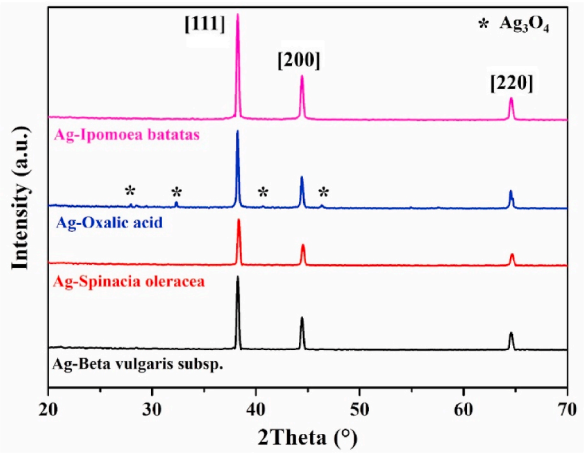

Fig. 2. X- XRD patterns of AgNPs synthesized with Oxalic acid, *Ipomoea batatas*, *Spinacia oleracea,* and *Beta vulgaris* subsp. as chelating fuels.

3. Results and discussion

3.1. Crystal structure analysis

The crystalline nature of the AgNPs synthesized by chemical and semi-organic combustion was confirmed by XRD analysis as shown in Fig. 2. Three distinct reflexes were observed at 38.22° (111), 44.45° (200), and 64.65° (220) for AgNPs synthesized with each chelating fuel, thus confirming the successful synthesis of AgNPs with a chemical chelating agent (oxalic acid) and organic chelating agents (*Ipomoea batatas, Spinacia oleracea* and *Beta vulgaris* subsp.). The XRD patterns further confirmed the face-centered cubic structure of AgNPs (*JCPDS file No. 04–0783)* [27]. XRD patterns revealed the presence of AgNPs as the main phase in all samples. However, a secondary phase also appeared for AgNPs synthesized with oxalic acid as the chelating fuel. The additional reflexes observed at the 2θ (hkl) values close to 28°, 33°, 42° and 47° come from the silver oxide, Ag_3O_4 (*JCPDS file No. 00-040-1054*), present on the surface of the silver nanoparticles [28]. In contrast to the reports of many researchers where the presence of many secondary phases was found in green-synthesized AgNPs [29,30], in our study only a small amount of secondary phase appeared in the sample synthesized using oxalic acid as a chelating agent. The average crystallite size of AgNPs calculated using the Scherrer equation for all samples was in the range of 17–21 nm illustrating their nano-dimensionality [31,32].

3.2. Microstructural and elemental analysis

Fig. 3(a–h), represents the FESEM micrographs of AgNPs synthesized by chemical and semi-organic combustion routes. The micrographs depict the morphology, size, and degree of agglomeration of the AgNPs. It is clear from all micrographs that AgNPs synthesized by all chelating fuels exhibit spherical shapes with average sizes of 150–250 nm and are poly-dispersed. Fig. 3(a and b) also shows that AgNPs synthesized using oxalic acid are uniform and form a network structure with each other, unlike AgNPs synthesized using organic extracts as chelating fuel. Fig. 3(c-h) shows expanded agglomerations and densification of the AgNPs with each other, which can be attributed to the formation of carbonate resulting from organic extracts of *Beta vulgaris* subsp., *Ipomoea batatas* and *Spinacia oleracea* have melted and diffused during the sintering process, causing agglomeration and densification. It was found that most carbonates begin to melt at 720 °C, while the decomposition of carbonate occurs at temperatures above 800 °C [33,34]. Since AgNPs are sintered at 750 °C, it is more likely that these carbonates melt and diffuse between particles, thus causing densification and agglomeration. The elemental analysis of AgNPs synthesized with different chelating fuels (*Oxalic acid, Beta vulgaris* subsp., *Spinacia oleracea*, and *Ipomoea batatas*.) are shown in Figs. S1, S2, S3, and S4 respe ctively.

The TEM micrographs shown in Fig. 4(a-l) depict the morphology and dimensions of the AgNPs synthesized with chemical (*oxalic acid*) and organic chelating agents (*Beta vulgaris* subsp., *Ipomoea batatas* and *Spinacia oleracea)*. In the images, the dark colour represents the AgNPs while irregular light-coloured material is the organic component of the sample, and the lighter material of even contrast is the underlying carbon film of the TEM grids. In all samples, Ag particles are approximately spherical and their diameters range from around 3–5 nm up to 60–120 nm. In all cases, the majority of particles are of around 10 nm diameter or less. The crystal structure of the ~20 nm single-crystalline particle circled in Fig. 4(a-c) is aligned with the electron beam and so this part of the image can be used to calculate a digital diffraction pattern, which is inset. This can be indexed to the face-centered cubic structure of Ag, viewed along the (111) zone axis. It can be further observed from Fig. 4 (d-i) that AgNPs synthesized with organic chelating agents

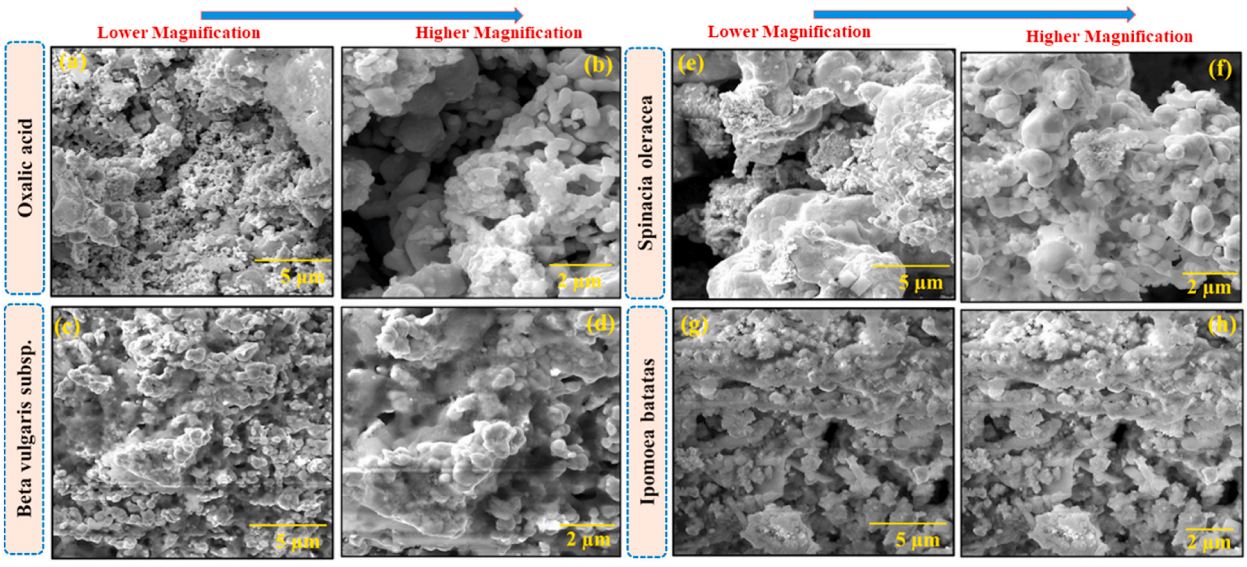

Fig. 3. SEM micrographs of AgNPs synthesized with different chelating fuels: **(a, b)** *Oxalic acid,* **(c, d)** *Beta vulgaris* subsp., **(e, f)** *Spinacia oleracea,* and **(g, h).** *Ipomoea batatas* at different magnifications.

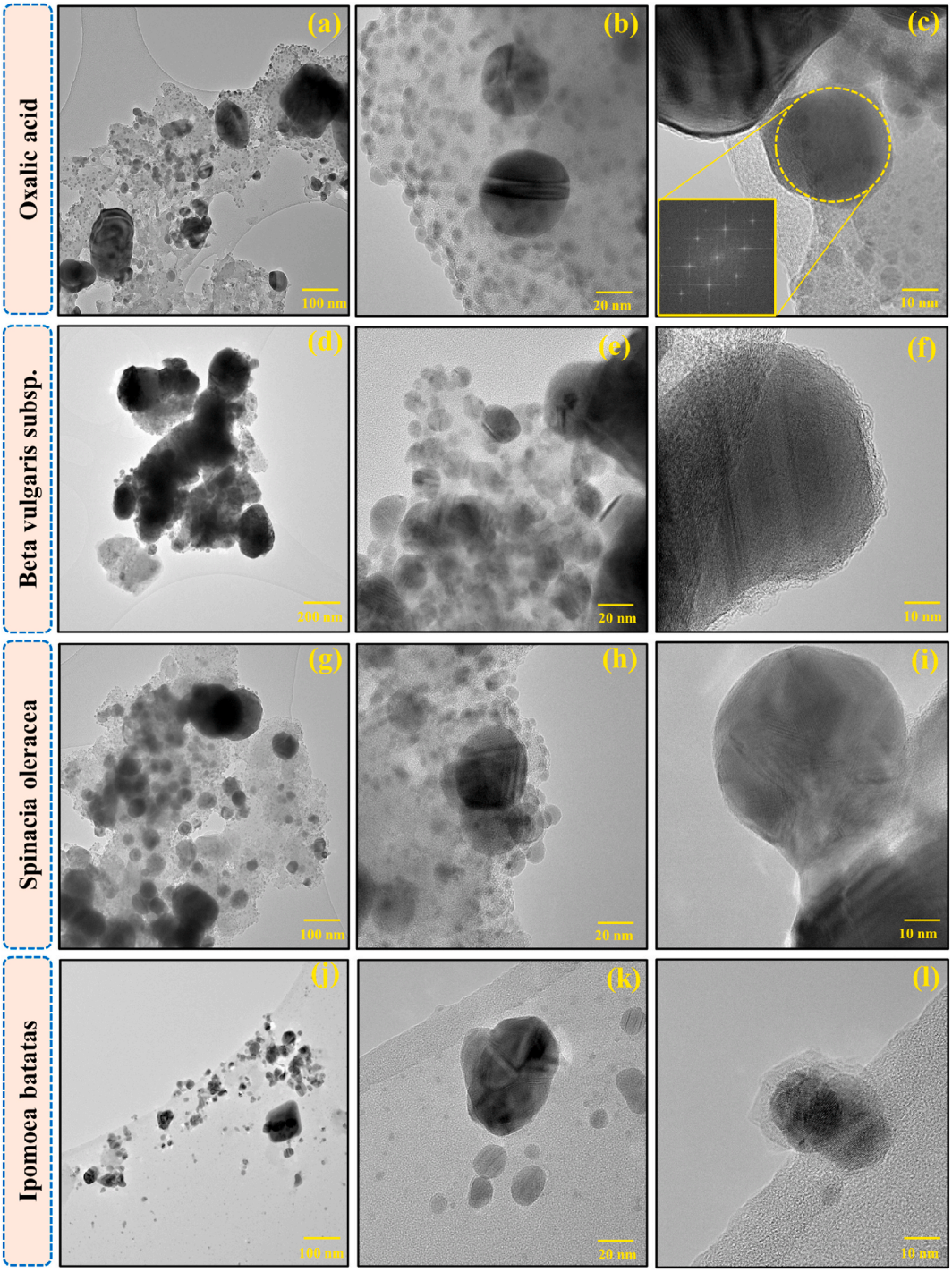

Fig. 4. TEM images at increasing magnifications for AgNPs synthesized with *Oxalic acid* **(a–c);** *Beta vulgaris* subsp. **(d–f);** *Spinacia oleracea* **(g–i);** and *Ipomoea batatas* **(j–l).** A digital diffraction pattern obtained from the particle indicated in **(c)** is inset and can be indexed to the face-centered cubic crystal structure of Ag viewed along the (111) zone axis.

exhibited more irregular light-coloured material due to the presence of a carbonate layer over the surface of particles, formed during the synthesis process. The decomposition of carbonate takes place at temperatures greater than 800 °C [34] and since the sintering temperature of AgNPs was kept at 750 °C, the irregular, light-coloured material observed in micrographs can be identified as likely being a carbonate layer [35]. It is also clear from Fig. 4(j-l) that AgNPs synthesized with organic chelating agents exhibited higher coagulation of the smaller particles than for AgNPs synthesized with oxalic acid. This can be attributed to different pH, or solvent

compositions due to the presence of terpenoids, alkaloids, phenolic compounds, glucosinolates, etc. [36].

3.3. XPS analysis

XPS studies can provide information on the elemental composition, the chemical bonds present on the surface, and the degrees of oxidation of individual elements. The XPS survey scans taken in the 0–1100 eV range showed that silver, oxygen, and carbon are present on samples surface and are accompanied by sodium and chlorine most likely as a residue from synthesis. The high-resolution spectra of Ag 3d, O 1s, and C 1s lines were used to analyze the chemical states of the AgNPs.

The Ag 3d XPS spectra of measured samples are presented in Fig. 5. In the case of the oxalic acid sample, the spectrum is fitted with three components centered at Ag $3d_{5/2}$ binding energy (BE) of 368.5, 369.8, and 372.6 eV. The first contribution is characteristic of the bulk-like metallic Ag (blue arrows), whereas the second component (magenta arrows) can be assigned to the metallic Ag nanoparticles. This is consistent with the well-known relationship of the binding energy of nanoparticles with their dimensions, that is, the larger the particles, the smaller their BE [37]. The third component (green arrows) with extremely high BE of 372.6 eV is related to the surface differential charging effect, which is due to the fact that the sample is not homogeneous. The effect of the presence of areas of different conductivity in AgNPs was widely discussed by Vasilkov et al. [38]. It is important to mention that the inhomogeneity of the samples prepared using the novel semi-organic combustion route is significantly higher than in samples using the chemical auto-combustion method, as manifested by a large increase of the component with the highest binding energy (Fig. 5(a)). The most heterogeneous AgNPs were prepared via spinach powder. Given that silver oxides are reported at Ag $3d_{5/2}$ BE of 367.7 eV (Ag_2O) and 367.3 eV (AgO) [39,40], it can be concluded that no oxidation of nanoparticles was detected in our measurements. The small contribution seen at the lowest BE values is associated with $K_{\alpha 3,4}$ satellites coming from a non-monochromatic X-ray source.

The O 1s core level spectra of AgNP prepared with different chelating agents are presented in Fig. 5(b). Three well-separated peaks at BE of 532.2, 533.8, and 535.3 eV were used to properly fit the spectra. The first component corresponds to the alkyl O atom of the –O-C=O group. The second signal may be assigned to C–*O*–C and/or C–OH groups [38]. The third contribution is related to the above-mentioned surface differential charging effect [41]. Predictably, the increase in the latter component goes hand in hand with an increase in the component with the highest BE on the Ag 3d spectrum. No components corresponding to silver oxides (529.4 eV for Ag_2O or 528.4 eV for AgO [39] are observed in the O 1s spectrum. It is noteworthy that there is a significant negative shift in the components with the lowest BE values in the beetroot sample.

Confirmation of the occurrence of the surface differential charging effect is best seen in C 1s spectra (Fig. 5(c)). In addition to the three characteristic components observed in the C 1s spectra of silver nanoparticles (marked by arrows), several additional signals shifted toward higher binding energies appeared. Characteristic contributions are related to the alkyl C–C/C–H (285.3 eV), C=O/O–C=O (287.7 eV), and C(O)O groups (291.0 eV) [38]. A sample prepared by the chemical route has a better conductivity, and thus the whole spectrum is slightly shifted toward lower binding energies. Moreover, in this sample, a component associated with C–O rather than C=O bonds can be discerned.

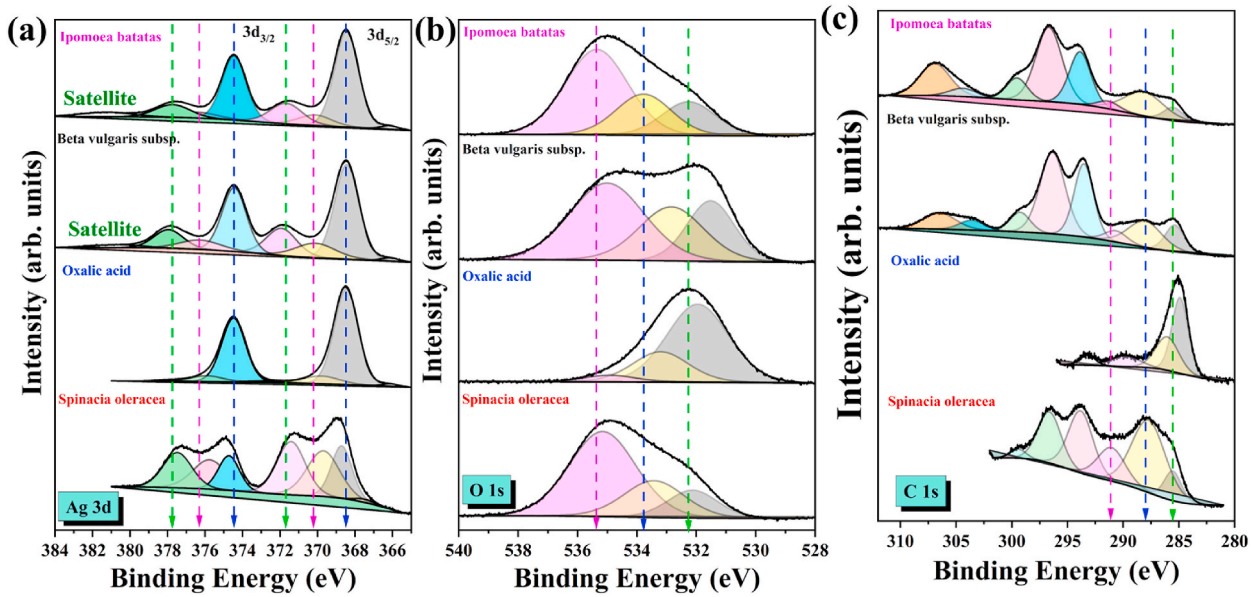

Fig. 5. The Ag 3d **(a);** O 1s **(b);** C 1s **(c);** XPS spectra of AgNPs.

3.4. Anti-bacterial study

The antimicrobial activity of AgNPs synthesized by chemical and semi-organic combustion methods and in combination with honey to inhibit the growth of *E. coli* bacteria was obtained by determining optical density (OD) using a spectrophotometer. The OD measurements against *E. coli* for 2g of mixture containing AgNPs (oxalic acid) + honey, AgNPs (*Beta vulgaris* subsp.) + honey, 2g of AgNPs (*Ipomoea batatas*) + honey, and AgNPs (*Spinacia oleracea*) honey, relative to the control positive and control negative control were plotted as a function of time and are shown in Fig. 6. Furthermore, honey is employed in conjunction with AgNPs to harness its exceptional antibacterial properties alongside those of AgNPs. Osmosis is a crucial factor in honey that has antibacterial effects against important disease-causing microbes. This is because honey is mostly made up of fructose and glucose, which cause dehydration of bacteria upon contact and prevent their development. The low water content in honey, which is less than 20 %, inhibits bacterial growth as bacteria depend on water for their metabolic activities. Furthermore, honey contains flavonoids, phenolic acids, and enzymes that exhibit phytochemical and antioxidant properties. The components of honey play a vital part in its antibacterial effect by counteracting free radicals [14–16]. Fig. 6(a-e) shows a graph of the OD values of the synthesized AgNPs, control positive, and control negative for 2 g of AgNPs combined with 1 g of honey. It is clear from the graph that AgNPs synthesized using *Spinacia oleracea* combined with honey showed the highest growth reduction of *E. coli.* when introduced into the culture medium for a period of 120 h compared to AgNPs synthesized using other chelating fuels. The OD values also show decrease in the control positive value after 96 h because the bacteria have started to die by their own waste developed in the culture medium. Furthermore, it can also be observed that some samples exhibited higher OD values than the control positive depicting the growth of the bacteria which can be attributed to the presence of carbonates in the AgNPs synthesized with organic chelating agents because *E. coli.* can grow in the presence of the carbonates. The TEM micrographs also confirmed the presence of layers of material, assigned as carbonate layers, for the sample synthesized with organic chelating agents. On the other hand, AgNPs synthesized with oxalic acid did not show this behavior due to the absence of carbonates. It is because low concentrations of carbonates can function as buffers, aiding in the regulation of the pH of the surrounding environment. *E. coli.* bacteria thrive and survive best within an optimal pH range, which is normally around neutral to slightly acidic environments. In addition, low concentration of carbonates can contribute to pH stabilization within this range, therefore facilitating the development of *E. coli.* under favourable circumstances [42,43]. Table 1 lists the reduction growth (%) of the *E.coli* in the culture medium supplemented with AgNPs (*Beta vulgaris* subsp., *Spinacia oleracea, Ipomoea batatas,* and oxalic acid) in combination with honey using equations (1) and (2). It can be observed from Table 1 that AgNPs synthesized using *Beta vulgaris* subsp., *Spinacia oleracea, Ipomoea batatas,* and oxalic acid showed a maximum growth reduction value of 51.1 %, 75.2 %, 67.8 %, and 55.4 %, respectively, against *E. coli.* over a period of 120 h. It is clear that AgNPs (*Spinacia oleracea, Ipomoea batatas)* exhibited better anti-bacterial activity against *E.coli* while AgNPs *(Beta vulgaris* subsp.*)* showed nearly the same antibacterial activity compared to AgNPs (oxalic acid) depicting that AgNPs synthesized organic chelating agents can be effectively utilized against *E. coli.* The better anti-bacterial activity of AgNPs (bio-based chelating agents) can be ascribed to metal impurities present in organic chelating agents

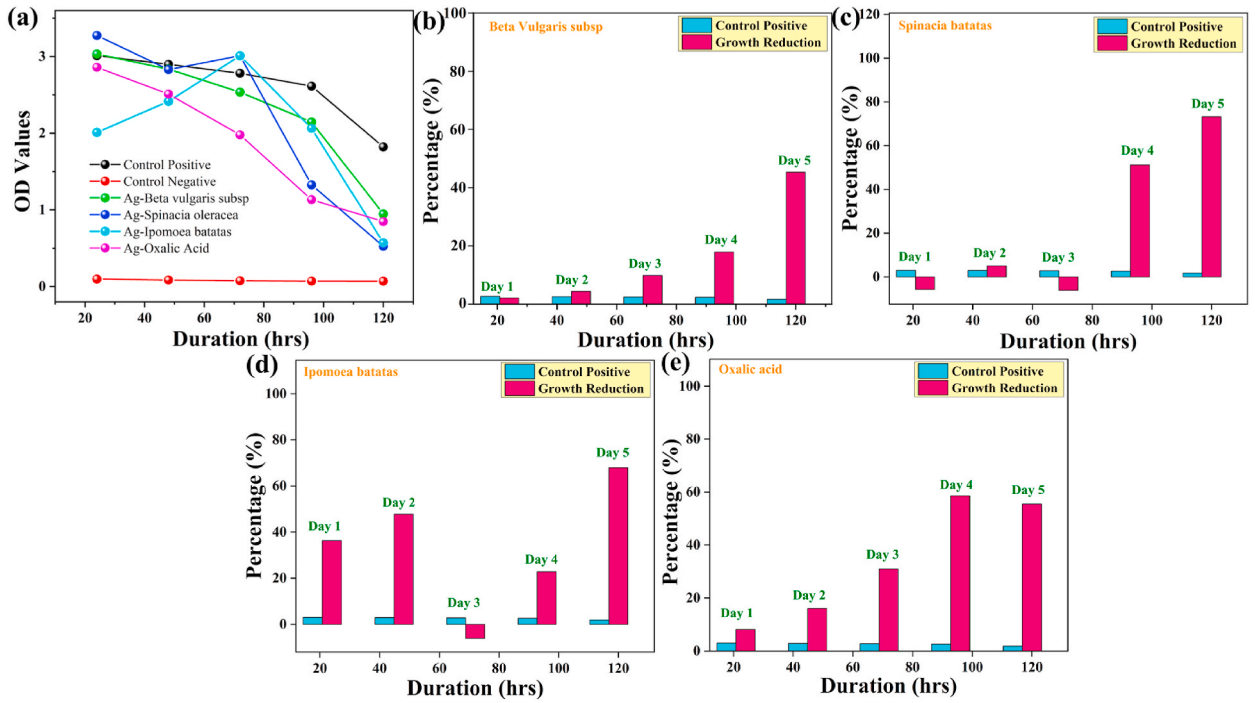

Fig. 6. OD values **(a)** and growth reduction **(b–e)** of AgNPs synthesized with *Ipomoea batatas, Beta vulgaris* subsp., *Spinacia oleracea* and synthetic oxalic acid.

Table 1
Reduction growth (%) of *E. coli.* with respect to time. **(**Control positive is LB solution with *E. coli.* while the control negative is LB solution without *E. coli.)*

Time (hrs)	Control Positive (C.P.)	Control Negative (C.N.)	Red. Growth *Ag-Beta Vulgaris* subsp (%)	Red. Growth *Ag-Spinacia oleracea* (%)	Red. Growth *Ag-Ipomoea batatas* (%)	Red. Growth Ag-oxalic acid (%)
24	3.012	0.091	2.3	−5.7	36.3	8.1
48	2.897	0.079	4.9	5.05	47.7	16.1
72	2.781	0.058	10.9	−6.1	−6.1	31
96	2.613	0.049	19.8	51.1	22.9	58.5
120	1.820	0.037	51.1	75.2	67.8	55.4

therefore combining their individual anti-bacterial properties with those of AgNPs. The mixture containing AgNPs (synthesized with *Spinacia oleracea*) showed better growth reduction. This can be related to the high levels of iron and manganese in spinach, which can impede bacterial growth by disrupting cell membranes, inducing oxidative stress, and interfering with cellular processes, ultimately resulting in bacterial demise. The antibacterial activity of mixture containing AgNPs + honey against *E. coli.* has not been reported to best of our knowledge, however several researchers have reported antibacterial activity against *E. coli* with greenly synthesized AgNPs using various testing techniques including broth dilution. Y. He et al. recorded a growth inhibition against *E. coli* of ~64 % through broth dilution technique for AgNPs synthesized using *Alpinia katsumadai* [44]. M. Baghayeri et al. used disk diffusion method and noted ~76.5 % *E. coli* growth inhibition for AgNPs synthesized with *Salvia leriifolia* [45]. Another group of researchers, used *Eucalyptus globulus* for synthesis of AgNPs and found a ~80 % growth reduction through broth dilution technique [46]. Similarly, AgNPs synthesized with *Bacillus thuringiensis* (96) reduced the viability of *E. coli* to ~45 % [47]. Researchers also found high antibacterial activity of AgNPs synthesized with *Enteromorpha exuosa* against *E. coli.* compared to chemically synthesized AgNPs depicting that biomolecules present in the bio-synthesized AgNPs can enhance the antibacterial activity of individual AgNPs [48]. It can be safely assumed that AgNPs synthesized with bio-based chelating agents can be successfully used in combination with honey against *E. coli.*

4. Conclusions

AgNPs were successfully synthesized with reduced impurities and ecological impact through a semi-organic pathway using bio-based chelating agents (*Ipomoea batatas, Spinacia oleracea, and Beta vulgaris* subsp. All synthesized AgNPs exhibited a cubic structure, confirming their crystalline nature. Notably, AgNPs synthesized through bio-based chelating agents exhibited denser structure compared to synthesized by synthetic oxalic acid. TEM micrographs showed AgNPs with typical diameters of 3–120 nm and a carbonate layer for the AgNPs synthesized with bio-based chelating agents while the elemental composition confirmed silver in all samples. XPS analysis revealed trace amount of Na and Cl on the surface of the samples, with notable residues of carbonates. The Ag 3d line analysis indicated the absence of oxides on the surface of the nanoparticles, affirming the purity of AgNPs. The antibacterial activity of synthesized AgNPs in combination with honey was evaluated against *E. coli*. The overalls growth reduction of 51–75 % is observed for all mixtures with the highest growth reduction (~75 %) observed for the mixture having AgNPs (*Ipomoea batatas*) and the least growth reduction (~51 %) for the mixture having AgNPs (Beta vulgaris subsp.). The study further concludes that semi-organic route provides a more environmentally friendly route for synthesizing AgNPs with reduced impurities. Moreover, AgNPs produced using organic chelating agents can be efficiently used in conjunction with honey for antibacterial purposes.

CRediT authorship contribution statement

Muneeb Irshad: Writing – review & editing, Writing – original draft, Visualization, Validation, Supervision, Software, Resources, Project administration, Methodology, Investigation, Funding acquisition, Formal analysis, Data curation, Conceptualization. **Anum Mukhtar:** Writing – review & editing, Writing – original draft, Visualization, Software, Investigation, Formal analysis, Data curation. **Asif Nadeem Tabish:** Writing – review & editing, Writing – original draft, Visualization, Supervision, Resources, Methodology, Investigation, Conceptualization. **Muhammad Bilal Hanif:** Writing – review & editing, Writing – original draft, Visualization, Validation, Supervision, Resources, Investigation, Funding acquisition, Formal analysis, Data curation. **Mahshab Sheraz:** Writing – review & editing, Writing – original draft, Visualization, Software, Project administration, Methodology, Investigation, Funding acquisition, Formal analysis. **Viktoriia Berezenko:** Writing – review & editing, Validation, Investigation, Formal analysis. **Muhammad Zubair Khan:** Writing – review & editing, Visualization, Software, Methodology, Investigation, Formal analysis. **Farwa Batool:** Writing – review & editing, Writing – original draft, Formal analysis, Data curation. **Muhammad Imran:** Writing – review & editing, Validation, Formal analysis, Data curation. **Muhammad Rafique:** Writing – original draft, Investigation, Funding acquisition, Formal analysis, Data curation. **Jacek Gurgul:** Writing – original draft, Visualization, Funding acquisition, Formal analysis, Data curation. **Thamraa Alshahrani:** Writing – original draft, Visualization, Funding acquisition, Formal analysis. **Michał Mosiałek:** Writing – review & editing, Visualization, Investigation, Funding acquisition. **Juran Kim:** Writing – review & editing, Writing – original draft, Visualization, Validation, Supervision, Software, Resources, Methodology, Investigation, Funding acquisition, Formal analysis, Data curation, Conceptualization. **Richard T. Baker:** Writing – review & editing, Validation, Supervision, Investigation, Formal analysis, Data curation. **Martin Motola:** Writing – review & editing, Visualization, Software, Resources, Methodology, Investigation, Funding acquisition, Formal analysis, Data curation.

Declaration of competing interest

The authors declare that they have no known competing financial interests or personal relationships that could have appeared to influence the work reported in this paper.

Acknowledgments

The authors are thankful for the financial support from the National Research Council of Science & Technology (NST) grant by the Korean government (MSIT) (No. CAP20022-000), Korea Institute of Industrial Technology (PUR24400) and the National Research Foundation of Korea (NRF-2021R1F1A1061200). The present work has been assisted by the project USCCCORD (ŽoNFP: NFP313020BUZ3), co-financed by the European Regional Development Fund within the Operational Programme Integrated Infrastructure. The work was also funded by the Grant of the Comenius University Bratislava for Young Scientists: UK/24/2023. TEM was performed at the Electron Microscopy Facility, University of St Andrews and we acknowledge support for the centre from the Engineering and Physical Sciences Research Council of the UK (EP/L017008/1, EP/R023751/1, and EP/T019298/1). We also want to acknowledge our work to Prof. Michał Mosiałek, who is the coauthor of this manuscript. He recently passed away before the publication of this manuscript.

Appendix A. Supplementary data

Supplementary data to this article can be found online at https://doi.org/10.1016/j.heliyon.2024.e31424.

References

[1] R. Kumar, M. Kumar, G. Luthra, Fundamental approaches and applications of nanotechnology: a mini review, Mater. Today Proc. (Jan. 2023), https://doi.org/10.1016/J.MATPR.2022.12.172.
[2] A.K. Verma, P. Kumar, On recent developments in biosynthesis and application of Au and Ag nanoparticles from biological systems, J. Nanotechnol. 2022 (2022), https://doi.org/10.1155/2022/5560244.
[3] C. An, et al., Nanomaterials and nanotechnology for the delivery of agrochemicals: strategies towards sustainable agriculture, J. Nanobiotechnol. 20 (1) (2022) 1–19, https://doi.org/10.1186/s12951-021-01214-7.
[4] P.L. Chee, W.L. Toh, P.Y. Yew, S. Peng, D. Kai, Chapter 1. Introduction of Nanotechnology and Sustainability, No. 57, 2022, https://doi.org/10.1039/9781839165771-00001.
[5] A. Haleem, M. Javaid, R.P. Singh, S. Rab, R. Suman, Applications of nanotechnology in medical field: a brief review, Glob. Health J 7 (2) (2023) 70–77.
[6] L. Zhang, Y. Jiang, Y. Ding, M. Povey, D. York, Investigation into the antibacterial behaviour of suspensions of ZnO nanoparticles (ZnO nanofluids), J. Nanoparticle Res. 9 (3) (2007) 479–489, https://doi.org/10.1007/s11051-006-9150-1.
[7] T. Bruna, F. Maldonado-Bravo, P. Jara, N. Caro, Silver nanoparticles and their antibacterial applications, Int. J. Mol. Sci. 22 (13) (2021), https://doi.org/10.3390/ijms22137202.
[8] O. Maťátková, J. Michailidu, A. Miškovská, I. Kolouchová, J. Masák, A. Čejková, Antimicrobial properties and applications of metal nanoparticles biosynthesized by green methods, Biotechnol. Adv. 58 (December 2021) (2022), https://doi.org/10.1016/j.biotechadv.2022.107905.
[9] M. Tariq, K.N. Mohammad, B. Ahmed, M.A. Siddiqui, J. Lee, Biological synthesis of silver nanoparticles and prospects in plant disease management, Molecules 27 (15) (2022), https://doi.org/10.3390/molecules27154754.
[10] A. Nicolae-maranciuc, D. Chicea, L.M. Chicea, Ag Nanoparticles for Biomedical Applications — Synthesis and Characterization — A Review, 2022.
[11] K. Jantakee, Y. Tragoolpua, Activities of different types of Thai honey on pathogenic bacteria causing skin diseases, tyrosinase enzyme and generating free radicals, Biol. Res. 48 (2015) 1–11.
[12] N. Bahari, N. Hashim, A. Md Akim, B. Maringgal, Recent advances in honey-based nanoparticles for wound dressing: a review, Nanomaterials 12 (15) (2022) 2560, https://doi.org/10.3390/nano12152560.
[13] R. Yaghoobi, A. Kazerouni, Evidence for clinical use of honey in wound healing as an anti-bacterial, anti-inflammatory anti-oxidant and anti-viral agent: a review, Jundishapur J. Nat. Pharm. Prod. 8 (3) (2013) 100.
[14] V. Hugo, et al., Comparison of the antibacterial effect of different biological silver nanoparticles synthetized and integrated with honeys 1 (1) (2022) 1–23, https://doi.org/10.55121/nefm.v1i1.46.
[15] M.L. Hossain, L.Y. Lim, K. Hammer, D. Hettiarachchi, C. Locher, A review of commonly used methodologies for assessing the antibacterial activity of honey and honey products, Antibiotics 11 (7) (2022), https://doi.org/10.3390/antibiotics11070975.
[16] I. Tanuwidjaja, et al., Chemical profiling and antimicrobial properties of honey bee (Apis mellifera l.) venom, Molecules 26 (10) (2021), https://doi.org/10.3390/molecules26103049.
[17] Y. Khane, et al., Green synthesis of silver nanoparticles using aqueous citrus limon zest extract: characterization and evaluation of their antioxidant and antimicrobial properties, Nanomaterials 12 (12) (2022), https://doi.org/10.3390/nano12122013.
[18] S.S. Abdulsahib, Synthesis, characterization and biomedical applications of silver nanoparticles, Biomedica 41 (2021) 458–464, https://doi.org/10.51248/.v41i2.1058.
[19] A.K. Sidhu, N. Verma, P. Kaushal, Role of biogenic capping agents in the synthesis of metallic nanoparticles and evaluation of their therapeutic potential, Front. Nanotechnol. 3 (Jan) (2022), https://doi.org/10.3389/FNANO.2021.801620/FULL.
[20] M. Danjuma, A. Adamu, S. K.-N, Eco-friendly synthesis and characterization of iron nanoparticles using crude extract from Eucalyptus globulus leaves as reducing and capping agents, Nanochemres.org 7 (2) (2022) 135–142. http://www.nanochemres.org/article_159683.html.
[21] A. Roy, O. Bulut, S. Some, A. Mandal, M.Y.-R. advances, Green Synthesis of Silver Nanoparticles: Biomolecule-Nanoparticle Organizations Targeting Antimicrobial Activity, pubs.rsc.org, 2019 undefined, https://pubs.rsc.org/en/content/articlehtml/2019/ra/c8ra08982e. (Accessed 16 May 2023).
[22] N.S. Alharbi, N.S. Alsubhi, A.I. Felimban, Green synthesis of silver nanoparticles using medicinal plants: characterization and application, J. Radiat. Res. Appl. Sci. 15 (3) (2022) 109–124, https://doi.org/10.1016/j.jrras.2022.06.012.
[23] J.R. Naik, M. David, Green synthesis of silver nanoparticles using Caesalpinia bonducella leaf extract: characterization and evaluation of in vitro anti-inflammatory and anti-cancer activities, Inorg. Nano-Metal Chem. 0 (0) (2022) 1–11, https://doi.org/10.1080/24701556.2021.2025093.
[24] R.F. Talabani, S.M. Hamad, A.A. Barzinjy, U. Demir, Biosynthesis of silver nanoparticles and their applications in harvesting sunlight for solar thermal generation, Nanomaterials 11 (9) (2021), https://doi.org/10.3390/nano11092421.

[25] M. Irshad, et al., Synergistic role of Biomolecules and Bio-chelating agents in the sustainable development of an efficient BaCe0. 97M0. 03O3-δ (M= Sm, Gd) perovskite electrolyte for IT-SOFC, Ceram. Int. 49 (23) (2023) 38360–38366.
[26] T. Dutta, S.K. Chowdhury, N.N. Ghosh, A.P. Chattopadhyay, M. Das, V. Mandal, Green synthesis of antimicrobial silver nanoparticles using fruit extract of Glycosmis pentaphylla and its theoretical explanations, J. Mol. Struct. 1247 (2022) 131361, https://doi.org/10.1016/j.molstruc.2021.131361.
[27] U.T. Khatoon, K.V. Rao, J.V.R. Rao, Y. Aparna, Synthesis and characterization of silver nanoparticles by chemical reduction method, in: International Conference on Nanoscience, Engineering and Technology (ICONSET 2011), 2011, pp. 97–99.
[28] M. Mohsin, M. Jawad, M.A. Yameen, A. Waseem, S.H. Shah, A.J. Shaikh, An insight into the coating behavior of bimetallic silver and gold core-shell nanoparticles, Plasmonics 15 (2020) 1599–1612.
[29] S. Gurunathan, J.W. Han, D.-N. Kwon, J.-H. Kim, Enhanced antibacterial and anti-biofilm activities of silver nanoparticles against Gram-negative and Gram-positive bacteria, Nanoscale Res. Lett. 9 (2014) 1–17.
[30] P.P.N. Vijay Kumar, S.V.N. Pammi, P. Kollu, K.V.V. Satyanarayana, U. Shameem, Green synthesis and characterization of silver nanoparticles using Boerhaavia diffusa plant extract and their anti bacterial activity, Ind. Crops Prod. 52 (2014) 562–566, https://doi.org/10.1016/j.indcrop.2013.10.050.
[31] M. Irshad, et al., Electrochemical evaluation of mixed ionic electronic perovskite cathode LaNi1-xCoxO3-δ for IT-SOFC synthesized by high temperature decomposition, Int. J. Hydrogen Energy 46 (17) (2021) 10448–10456, https://doi.org/10.1016/j.ijhydene.2020.09.180.
[32] N. Thirumagal, A.P. Jeyakumari, Structural, optical and antibacterial properties of green synthesized silver nanoparticles (AgNPs) using Justicia adhatoda L. leaf extract, J. Cluster Sci. 31 (2) (2020) 487–497.
[33] J. Yu, et al., Synthesis of carbon-doped KNbO3 photocatalyst with excellent performance for photocatalytic hydrogen production, Sol. Energy Mater. Sol. Cells 179 (2018) 45–56, https://doi.org/10.1016/j.solmat.2018.01.043.
[34] X. Yao, H. Zhou, K. Xu, Q. Xu, L. Li, Investigation on the fusion characterization and melting kinetics of ashes from co-firing of anthracite and pine sawdust, Renew. Energy 145 (2020) 835–846.
[35] J. Walton, Aerosol damage to a microchannel plate analysed by X-ray photoelectron spectromicroscopy, Surf. Interface Anal. An Int. J. devoted to Dev. Appl. Tech. Anal. surfaces, interfaces thin Film 39 (4) (2007) 337–342.
[36] S.A. Mir, A. Manickavasagan, M.A. Shah, Plant Extracts: Applications in the Food Industry, Elsevier Science, 2021 [Online]. Available: https://books.google.com.pk/books?id=aJlSEAAAQBAJ.
[37] I. Lopez-Salido, D. Lim, Y.K.-S. science, Ag Nanoparticles on Highly Ordered Pyrolytic Graphite (HOPG) Surfaces Studied Using STM and XPS, Elsevier, 2005 undefined, https://www.sciencedirect.com/science/article/pii/S0039602805005376. (Accessed 30 April 2023).
[38] Plasmon resonance of silver nanoparticles as a method of increasing their antibacterial action," mdpi.com, Accessed: April. 30, 2023. [Online]. Available: https://www.mdpi.com/330270.
[39] M.A. Garcia, et al., Photoluminescence of silver in glassy matrices, J. Appl. Phys. 96 (7) (2004) 3737–3741.
[40] G.B. Hoflund, Z.F. Hazos, G.N. Salaita, Surface characterization study of Ag, AgO, and Ag2O using x-ray photoelectron spectroscopy and electron energy-loss spectroscopy, Phys. Rev. B Condens. Matter 62 (16) (Oct. 2000) 11126–11133, https://doi.org/10.1103/PHYSREVB.62.11126.
[41] V. Ambrogi, et al., Chitosan films containing mesoporous SBA-15 supported silver nanoparticles for wound dressing, J. Mater. Chem. B 2 (36) (Aug. 2014) 6054–6063, https://doi.org/10.1039/C4TB00927D.
[42] C. Merlin, M. Masters, S. McAteer, A. Coulson, Why is carbonic anhydrase essential to Escherichia coli? J. Bacteriol. 185 (21) (2003) 6415–6424.
[43] M.B. Farhangi, A.A.S. Sinegani, M.R. Mosaddeghi, A. Unc, G. Khodakaramian, Impact of calcium carbonate and temperature on survival of Escherichia coli in soil, J. Environ. Manag. 119 (2013) 13–19.
[44] Y. He et al., "Green synthesis of silver nanoparticles using seed extract of Alpinia katsumadai, and their antioxidant, cytotoxicity, and antibacterial activities," pubs.rsc.org, Accessed: May 17, 2023. [Online]. Available: https://pubs.rsc.org/en/content/articlehtml/2017/ra/c7ra05286c.
[45] M. Baghayeri, B. Mahdavi, Z. Hosseinpor-Mohsen Abadi, S. Farhadi, Green synthesis of silver nanoparticles using water extract of Salvia leriifolia: antibacterial studies and applications as catalysts in the electrochemical detection of nitrite, Appl. Organomet. Chem. 32 (2) (Feb. 2018), https://doi.org/10.1002/AOC.4057.
[46] K. Ali, B. Ahmed, S. Dwivedi, Q. Saquib, A.A. Al-Khedhairy, J. Musarrat, Microwave accelerated green synthesis of stable silver nanoparticles with Eucalyptus globulus leaf extract and their antibacterial and antibiofilm activity on clinical isolates, PLoS One 10 (7) (Jul. 2015), https://doi.org/10.1371/JOURNAL.PONE.0131178.
[47] P. Sarthi Nayak, M. Arakha, A. Kumar, S. Asthana, B. C. Mallick, and S. Jha, "An approach towards continuous production of silver nanoparticles using Bacillus thuringiensis," pubs.rsc.org, Accessed: May 17, 2023. [Online]. Available: https://pubs.rsc.org/en/content/articlehtml/2016/ra/c5ra21281b.
[48] M. Yousefzadi, Z. Rahimi, V.G.-M. Letters, The Green Synthesis, Characterization and Antimicrobial Activities of Silver Nanoparticles Synthesized from Green Alga Enteromorpha Flexuosa (Wulfen) J, Elsevier, 2014 and undefined, https://www.sciencedirect.com/science/article/pii/S0167577X14015870?casa_token=ZDqnrcli7V0AAAAA:z5Izrl4qTJcU7UkwRMudsqN_9iRLhMDDeGXEygjmDZuqcS4ZcjgwTrYhYRcWMdy6MC4Rb7ac6ydD. (Accessed 17 May 2023).